

Silicon Mirrors for High-Intensity X-Ray Pump and Probe Experiments

Tom Pardini,^{1,*} Sébastien Boutet,² Joseph Bradley,^{1,†} Tilo Döppner,¹ Luke B. Fletcher,^{3,‡} Dennis F. Gardner,⁴ Randy M. Hill,¹ Mark S. Hunter,¹ Jacek Krzywinski,² Marc Messerschmidt,² Arthur E. Pak,¹ Florian Quirin,⁵ Klaus Sokolowski-Tinten,⁵ Garth J. Williams,² and Stefan P. Hau-Riege¹

¹Lawrence Livermore National Laboratory, Livermore, California 94550, USA

²SLAC National Accelerator Laboratory, Menlo Park, California 94025, USA

³Physics Department, University of California, Berkeley, California 94720, USA

⁴JILA, University of Colorado, 440 UCB, Boulder, Colorado 80309-0440, USA

⁵Faculty of Physics and Center for Nanointegration Duisburg-Essen (CENIDE), 47048 Duisburg, Germany

(Received 5 March 2014; revised manuscript received 7 May 2014; published 28 May 2014)

An all-x-ray pump and probe capability is highly desired for the free-electron laser community. A possible implementation involves the use of an x-ray mirror downstream of the sample to backreflect the pump beam onto itself. We expose silicon single crystals, a candidate for this hard-x-ray mirror, to the hard-x-ray beam of the Linac Coherent Light Source (SLAC National Acceleration Laboratory) to assess its suitability. We find that silicon is an appropriate mirror material, but its reflectivity at high x-ray fluences is somewhat unpredictable. We attribute this behavior to x-ray-induced local damage in the mirror, which we have characterized *post mortem* via microdiffraction, scanning electron microscopy, and Raman spectroscopy. We demonstrate a strategy to reduce local damage by using a structured silicon-based mirror. Preliminary results suggest that the latter yields reproducible Bragg reflectivity at high x-ray fluences, promising a path forward for silicon single crystals as x-ray backreflectors.

DOI: 10.1103/PhysRevApplied.1.044007

I. INTRODUCTION

X-ray free-electron lasers (XFELs) continue to be built around the world at an impressive pace. Their ability to deliver ultrabright photon bunches in the femtosecond regime allows experimentalists to probe physical processes on a time scale not accessible before. XFEL applicability ranges from high-energy density science (HEDS) and warm dense matter (WDM) [1,2] to biology [3–5] and solid state physics [6–8]. In these fields, XFELs are ideal probes given the abundant signal they provide despite the intrinsic weakness of the scattering process. At the same time, x rays are efficiently absorbed, which makes XFELs ideal tools to pump systems in unexplored high-energy states. A case in point are WDM states, where the need for an isochoric and isothermal transition is paramount. Combining the pump and probe capabilities of XFELs would provide unprecedented means to study material properties and dynamics under extreme conditions. Such capability would shed light on fundamental concepts in HEDS, including the mechanisms leading to x-ray-induced damage in materials.

Over the course of recent years, several attempts have been made to achieve pump and probe capabilities at an XFEL. One technique was demonstrated by Chapman and co-workers [9] for extreme-ultraviolet (EUV) light at FLASH (Free-Electron

Laser in Hamburg). Here, an EUV beam pumps a highly transmissive sample, then impinges on a multilayer mirror where it gets backreflected before it has time to destroy the mirror's local structure, and finally probes the same sample volume. Since the multilayer is locally damaged, a different part of the mirror is used for every shot. The delay between pump and probe can be dialed in by varying the distance between the sample and multilayer mirror.

Existing pump and probe techniques such as two-color seeding [10] and double-slotted spoilers [11,12] have low pump intensities, and the delay times are currently limited to 100 fs. Our goal is to develop a technique similar to that of Chapman and co-workers for the hard-x-ray regime using crystals as backreflectors. Multilayer mirrors in backscattering geometry cannot be used due to the short wavelength of the light. This restriction poses unique challenges: Reflections from single crystals are generally weak, but this weakness can be tolerated given the large brightness of the XFEL beam. More troublesome is the significant amount of ionization and atomic displacement generated in the crystal during the pulse, which results in a degradation of the Bragg signal [13,14]. This effect is particularly strong in single crystals compared to multilayers [9,15], given the large impact small atomic motion has on the interference effect leading to the formation of narrow Bragg peaks. However, with a single and sufficiently short pulse, it is possible to outpace radiation damage and to obtain Bragg reflection before the crystal structure is destroyed.

*pardini2@llnl.gov

†Present address: Amazon.com, Seattle, WA 98109, USA.

‡Present address: SLAC National Accelerator Laboratory, Menlo Park, CA 94566, USA.

In this paper, we investigate a silicon single crystal as a candidate for a hard-x-ray backreflector. While our data suggest that silicon can in fact backreflect intense beams at hard-x-ray energies, we also discover serious material issues related to memory effects that need to be addressed. In this paper, we discuss our findings and provide a path forward to circumvent these issues.

II. METHODS

The measurements reported in this paper are performed at the Linac Coherent Light Source (LCLS) Coherent X-ray Imaging (CXI) beam line [16,17]. A schematic view of the experimental setup is shown in Fig. 1. We place 500- and 100- μm -thick silicon (100) wafers in the focal plane of CXI's experimental chamber and expose them to 9.1-keV photon pulses with approximately 1.25-mJ pulse energy. Single-shot mode is chosen to irradiate the sample, with an approximately one second interval between successive shots. The beam energy bandwidth is approximately 0.2%, which implies that the contribution to silicon damage from the part of the beam that is Bragg reflected (approximately 10^{-5}) is small compared to the rest of the beam. Silicon attenuators are used to vary the beam transmission (T) in the range 8%–100%. The x-ray FWHM at focus is estimated to be $4 \pm 0.5 \mu\text{m}$ by using Liu's method [18] and agrees well with ray-tracing estimates. A photodiode placed upstream of the silicon mirror monitors the intensity of the (008) Bragg reflection for alignment purposes. The x-ray microdiffraction (XRMD) data shown in this paper are taken *post mortem* at LLNL by using a Panalytical X'Pert Pro diffractometer equipped with a Cu $K\alpha$ source and a 25- μm -diameter pinhole. We estimate the x-ray footprint on the sample (FWHM) to be approximately $100 \mu\text{m} \times 40 \mu\text{m}$ along the horizontal and vertical axes, respectively. This result is estimated first via ray tracing and confirmed experimentally by measuring the Bragg signal across a sharp sample edge. Alignment of the x-ray spot on the sample is obtained by detecting fluorescence from a reference phosphor screen with an optical alignment microscope and is estimated to be better than $\pm 25 \mu\text{m}$.

III. Si REFLECTORS AT HIGH X-RAY FLUENCE

Bragg reflectivity at high x-ray intensities has been the subject of several studies over the past few years: Hau-Riege and co-workers [1] expose graphite to the LCLS beam and measure the reflectivity up to a fluence

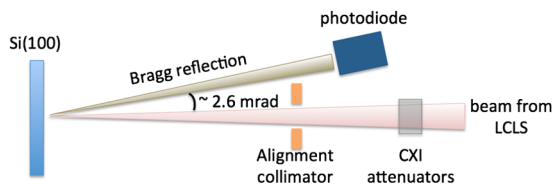


FIG. 1. Schematic view of the experimental configuration.

of $1.0 \text{ kJ}/\text{cm}^2$; Chapman and co-workers [19] demonstrate Bragg reflectivity in nanocrystals of photosystem I at $0.9 \text{ kJ}/\text{cm}^2$. Data collected in this study suggest that the Bragg reflectivity from single-crystal silicon is finite at least up to an x-ray fluence of $5.5 \text{ kJ}/\text{cm}^2$. Saturation of our photodiode does not allow us to quantify the actual amount of reflectivity achieved; nevertheless, a nonzero reflectivity at such high x-ray fluence is quite remarkable if we consider the amount of x-ray-induced damage after a shot. Figure 2(a) shows the crater created by a full fluence shot on a 500- μm -thick silicon (100) wafer. The diameter of the crater center visible in this scanning electron microscopy (SEM) image measures approximately $15 \mu\text{m}$. Extensive damage is usually observed in its vicinity up to a distance of approximately $100 \mu\text{m}$. Additionally, cracks can be seen to extend beyond this point, a feature not present in damage from vacuum-ultraviolet radiation where heat deposited on the surface tends to cause clean ablation without cracking. These data are in agreement with that observed by Koyama *et al.* [20] and already imply that, in order to achieve reproducible Bragg reflectivity in single-crystal silicon, the spacing between successively probed locations should be greater than several hundred microns, which is a considerable waste of sample surface. In order to get a more quantitative measure of the damage, the Bragg signal from a lineout across the same crater is collected with our microdiffractometer and shown in Fig. 2(b). The small footprint of the x-ray beam allows us to resolve individual craters, since in this example the closest neighboring crater is 1 mm away. The crater center corresponds to $x = 0 \text{ mm}$; a very limited Bragg signal is

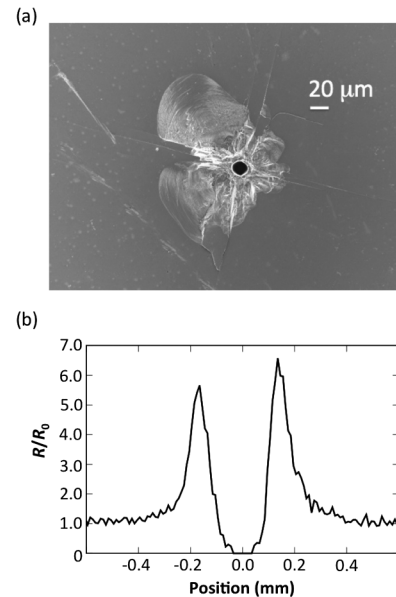


FIG. 2. SEM image of a crater in 500- μm -thick silicon (100) induced by an LCLS shot at full fluence (a). Bragg signal measured via XRMD along a lineout across the crater (b). Intensity is normalized to the single-crystal silicon reflectivity R_0 .

measured near the center, where Raman and XRMD analysis suggest the presence of a polycrystalline region subject to compressive stress and misalignment with respect to the undamaged crystal structure. On both sides of the crater, the Bragg signal is regained approximately $180\ \mu\text{m}$ from the crater center; this distance is considerable given the size of the crater. We point out that the magnitude of the integrated signal is more than 6 times *larger* than its baseline, the latter representing Bragg reflectivity of undamaged silicon. We conclude that the integrated reflectivity is enhanced by damage to the crystal structure not visible under SEM. We speculate that this damage is consistent with stressed micrograins (mosaicity), which break the perfect symmetry of the crystal structure and therefore relax the strict condition imposed to the Bragg reflection by the dynamical diffraction theory. In fact, for a perfect Si(100) crystal, only planes within the x-ray extinction depth (approximately $4.3\ \mu\text{m}$ at this energy) can contribute to Bragg reflection, and only a small spectral component of the incoming light is reflected. As the symmetry is broken, multiple mosaic elements within the approximately $100\text{-}\mu\text{m}$ x-ray attenuation length can contribute to the Bragg signal [21], while at the same time the spectral response of the crystal is increased, therefore enhancing the measured Bragg intensity.

To further deepen our understanding of x-ray-induced damage in single-crystal silicon, we apply microdiffraction analysis to craters generated by LCLS shots at different values of x-ray fluence. Figure 3 shows the Bragg signal measured along a lineout crossing five of these craters. The signal is normalized to the undamaged single-crystal signal. In this figure, x-ray fluence increases from left to right and is 0.8 (E), 1.4 (D), 2.6 (C), 5.5 (B), and 10.0 (A) kJ/cm^2 . The minima in the signal correspond to the crater locations (for the low fluence crater E, the diffractometer's beam size is too large to actually resolve the crater itself). The peaks correspond to regions of enhanced reflectivity, while reflectivity of unperturbed single-crystal silicon is visible in between craters. From the data it is clear that x-ray-induced

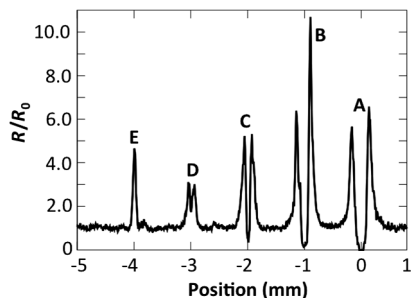


FIG. 3. Bragg signal measured via XRMD across five craters generated by LCLS shots at variable x-ray fluence: 0.8 (E), 1.4 (D), 2.6 (C), 5.5 (B), and 10.0 (A) kJ/cm^2 . Intensity is normalized to the single-crystal silicon reflectivity R_0 . Additionally, a baseline is removed from the data.

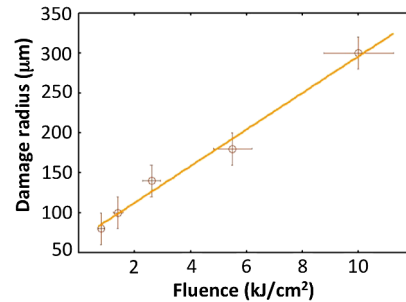


FIG. 4. Radius of the damaged area around a crater as a function of x-ray fluence with the corresponding linear fit.

damage enhances the reflectivity near a crater even at the lowest fluence investigated ($0.8\ \text{kJ}/\text{cm}^2$). While the spatial extent of the damage in the vicinity of a crater appears to be linear with fluence, its magnitude can be highly nonuniform as shown by the asymmetry in the signal near crater B in Fig. 3. Nevertheless, from these measurements it is possible to quantitatively correlate x-ray fluence with the extent of the damage in the vicinity of a crater and provide the minimum distance between successive exposures that would yield single-crystal Bragg reflectivity. A linear relation between radius and fluence is found, and a summary of this result is reported in Fig. 4.

To conclude this analysis, we mention that exposing a $100\text{-}\mu\text{m}$ -thick silicon wafer to the LCLS beam at full fluence results in sample cracking so severe that the sample has to be discarded after only a few shots, and no further analysis was attempted.

It would appear that in order to implement silicon as a mirror for high-intensity x rays only two options are available: (i) Either the spacing between successive shots is kept small to save the sample surface, in which case the Bragg reflectivity is hardly reproducible due to extensive local damage, or (ii) the spacing between shots is increased to several hundred microns, severely limiting the number of XFEL shots for a given mirror size.

In the following section, we propose an alternative option that promises to yield very reproducible values of reflectivity of spatially closely placed exposures, by confining the extent of the damage region.

IV. SILICON PILLARS AS HARD-X-RAY BACKREFLECTORS

Here we propose a prototype sample that can be implemented as an effective hard-x-ray backreflector. The idea is to circumvent extended damage inflicted by the LCLS beam on bulk silicon by using isolated silicon pillar reflectors that have intrinsically the same crystallographic alignment. A SEM image of a prototype sample is shown in Fig. 5.

This prototype is fabricated from 1-mm-thick silicon wafers and exposed to the LCLS beam. We fabricate the pillar samples by deep etching trenches in a single-crystal

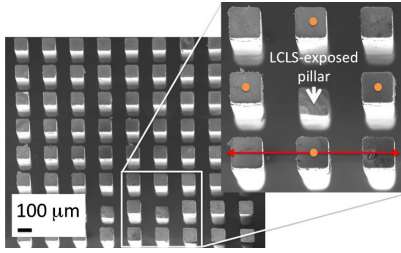


FIG. 5. SEM image of pillar structure: Pillars are $100\ \mu\text{m}$ wide and separated by $100\ \mu\text{m}$. (Inset) Enlarged view of the LCLS-exposed pillar and neighboring pillars; the red arrow indicates the direction of XRMD lineout shown in Fig. 6(a), while the orange dots represent the locations of Bragg reflectivity measurements shown in Fig. 6(b).

silicon wafer, resulting in pillars that are $650\ \mu\text{m}$ tall, $100\ \mu\text{m}$ wide, and separated by $100\ \mu\text{m}$. Since the pillars are all part of the same silicon wafer, they are all aligned with respect to each other. It would be possible to ion implant the silicon substrate to create depth grading, thereby broadening the reflectivity curve. We expose the pillars to 7.3-keV LCLS radiation at 1.25 mJ, focused to 200 nm. The x-ray transmission is 100%. We find that approximately 250–300 μm of each exposed pillar are obliterated, as seen in Fig. 5. Since the depth of the obliterated pillar is much larger than the x-ray penetration depth at 7.3 and 9.1 keV, the magnitude of the pulse energy is likely to determine the degree of the damage. The same pulse energy is used for the pillar and the single-crystal

experiments, so we believe that the pillar results at 7.3 keV are indicative of what we would expect at 9.1 keV. After the exposure, we use XRMD to verify that damage to a particular pillar does not affect the reflectivity of neighboring pillars. Figure 6(a) shows the Bragg reflectivity along a lineout crossing three pillars neighboring an LCLS-exposed pillar; Fig. 6(b) shows the Bragg curve collected on the four pillars neighboring the LCLS-exposed pillar. These data show that the signal is very reproducible in both intensity and position. We note that the self-amplified spontaneous emission operation mode is expected to produce stochastic variations in reflected intensity, since the spectral intensity of a SLAC pulse is fluctuating. A seeded beam will provide more reproducible values, at a somewhat lower intensity. In summary, we prove that the pillar concept works for our experiment and that a $100\text{-}\mu\text{m}$ pillar size is suitable to maximize the number of pillars (exposures) while maintaining mechanical integrity. Our setup allows two-color pump and probe experiments by reflecting a higher harmonic of the XFEL beam.

V. CONCLUSIONS

We have shown that single-crystal silicon can reflect high-intensity x rays from a hard-x-ray FEL. While the Bragg reflectivity is hardly reproducible due to x-ray damage, we propose the use of silicon pillars to circumvent this problem. Preliminary data collected at the LCLS show a path forward for silicon as a backreflector for hard x rays.

ACKNOWLEDGMENTS

T. P. thanks Todd Decker and Jennifer Alameda for their help with XRMD. We thank Ilme Schlichting for experimental support. F. Q. and K. S. T. acknowledge support by the German Research Council (DFG) through the Collaborative Research Centre SFB 616 “Energy Dissipation at Surfaces.” Portions of this research were carried out at the Linac Coherent Light Source (LCLS) at the SLAC National Accelerator Laboratory. LCLS is an Office of Science User Facility operated for the U.S. Department of Energy Office of Science by Stanford University. This work was performed under the auspices of the U.S. Department of Energy by Lawrence Livermore National Laboratory under Contract No. DE-AC52-07NA27344. Document Release No. LLNL-JRNL-649072.

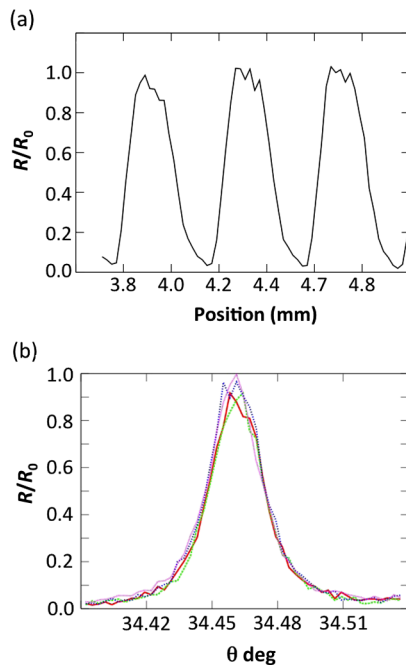


FIG. 6. XRMD lineout across three pillars neighboring the LCLS-exposed pillar (a); Bragg peak measured on the four pillars neighboring the LCLS-exposed pillar (b).

- [1] S. P. Hau-Riege, A. Graf, T. Döppner, R. A. London, J. Krzywinski, C. Fortmann, S. H. Glenzer, M. Frank, K. Sokolowski-Tinten, M. Messerschmidt, C. Bostedt, S. Schorb, J. A. Bradley, A. Lutman, D. Rolles, A. Rudenko, and B. Rudek, Ultrafast transitions from solid to liquid and plasma states of graphite induced by x-ray free-electron laser pulses, *Phys. Rev. Lett.* **108**, 217402 (2012).

- [2] O. Ciricosta *et al.*, Direct measurements of the ionization potential depression in a dense plasma, *Phys. Rev. Lett.* **109**, 065002 (2012).
- [3] H. N. Chapman *et al.*, Femtosecond x-ray protein nanocrystallography, *Nature (London)* **470**, 73 (2011).
- [4] A. V. Martin *et al.*, Single particle imaging with soft x-rays at the linac coherent light source, *Proc. SPIE Int. Soc. Opt. Eng.* **8078**, 807809 (2011).
- [5] L. Lomb *et al.*, Radiation damage in protein serial femtosecond crystallography using an x-ray free-electron laser, *Phys. Rev. B* **84**, 214111 (2011).
- [6] L. B. Fletcher, E. Galtier, H. J. Heimann, P. Lee, B. Nagler, J. Welch, U. Zastra, J. B. Hastings, and S. H. Glenzer, Plasmon measurements with a seeded x-ray laser, *JINST* **8**, C11014 (2013).
- [7] M. Trigo, M. Fuchs, J. Chen, M. P. Jiang, M. Cammarata, S. Fahy, D. M. Fritz, K. Gaffney, S. Ghimire, A. Higginbotham, S. L. Johnson, M. E. Kozina, J. Larsson, H. Lemke, A. M. Lindenberg, and G. Ndabashimiye, Fourier-transform inelastic x-ray scattering from time- and momentum-dependent phonon-phonon correlations, *Nat. Phys.* **9**, 790 (2013).
- [8] S. L. Johnson *et al.*, Femtosecond dynamics of the collinear-to-spiral antiferromagnetic phase transition in CuO, *Phys. Rev. Lett.* **108**, 037203 (2012).
- [9] H. N. Chapman *et al.*, Femtosecond time-delay x-ray holography, *Nature (London)* **448**, 676 (2007).
- [10] Giovanni De Nino, Benoît Mahieu, Enrico Allaria, Luca Giannessi, and Simone Spampinati, Chirped seeded free-electron lasers: Self-standing light sources for two-color pump-probe experiments, *Phys. Rev. Lett.* **110**, 064801 (2013).
- [11] Y. Ding, F.-J. Decker, P. Emma, C. Feng, C. Field, J. Frisch, Z. Huang, J. Krzywinski, H. Loos, J. Welch, J. Wu, and F. Zhou, Femtosecond x-ray pulse characterization in free-electron lasers using a cross-correlation technique, *Phys. Rev. Lett.* **109**, 254802 (2012).
- [12] P. Emma, K. Bane, M. Cornacchia, Z. Huang, H. Schlarb, G. Stupakov, and D. Walz, Femtosecond and subfemtosecond x-ray pulses from a self-amplified spontaneous-emission-based free-electron laser, *Phys. Rev. Lett.* **92**, 074801 (2004).
- [13] W. Wierzchowski *et al.*, Investigation of damage induced by intense femtosecond xuv pulses in silicon crystals by means of white beam synchrotron section topography, *Radiat. Phys. Chem.* **93**, 99 (2013).
- [14] J. B. Pelka *et al.*, Damage in solids irradiated by a single shot of xuv free-electron laser: Irreversible changes investigated using x-ray microdiffraction, atomic force microscopy and Nomarski optical microscopy, *Radiat. Phys. Chem.* **78**, S46 (2009).
- [15] S. P. Hau-Riege *et al.*, Subnanometer-scale measurements of the interaction of ultrafast soft x-ray free-electron-laser pulses with matter, *Phys. Rev. Lett.* **98**, 145502 (2007).
- [16] P. Emma *et al.*, First lasing and operation of an angstrom-wavelength free-electron laser, *Nat. Photonics* **4**, 641 (2010).
- [17] S. Boutet and G. J. Williams, The Coherent X-Ray Imaging (CXI) instrument at the Linac Coherent Light Source (LCLS), *New J. Phys.* **12**, 035024 (2010).
- [18] J. M. Liu, Simple technique for measurements of pulsed Gaussian-beam spot sizes, *Opt. Lett.* **7**, 196 (1982).
- [19] H. N. Chapman *et al.*, Femtosecond x-ray protein nanocrystallography, *Nature (London)* **470**, 73 (2011).
- [20] Takahisa Koyama, Hirokatsu Yumoto, Yasunori Senba, Kensuke Tono, Takahiro Sato, Tadashi Togashi, Yuichi Inubushi, Tetsuo Katayama, Jangwoo Kim, Satoshi Matsuyama, Hidekazu Mimura, Makina Yabashi, Kazuto Yamauchi, Haruhiko Ohashi, and Tetsuya Ishikawa, Investigation of ablation thresholds of optical materials using 1- μm -focusing beam at hard x-ray free electron laser, *Opt. Express* **21**, 15382 (2013).
- [21] W. H. Zachariassen, *Theory of X-ray Diffraction in Crystals* (Dover Phoenix Editions, New York, 2004).